CrossMark

ORIGINAL PAPER

Cyclosophoraose/cellulose hydrogels as an efficient delivery system for galangin, a hydrophobic antibacterial drug

Daham Jeong · Hyun ki Kim · Jae-pil Jeong · Someshwar D. Dindulkar ·
Eunae Cho · Yung-Hun Yang · Seunho Jung

Abstract Highly water-soluble cyclosophoraose (Cys) has been recently used as a suitable complexation agent to enhance the solubility of drugs that are hardly water-soluble by molecular encapsulation via host–guest complexation. In this study, a novel Cys/cellulose hydrogel was prepared by cross-linking Cys and cellulose for efficient galangin delivery to improve antibacterial activity. Galangin was known to directly inhibit the activity of β-lactamase and to exhibit intrinsic antibacterial activity. The inhibition of β-lactamase by galangin was also known to enhance the eradication of a strain of methicillin-resistant *Staphylococcus aureus*. However, efficient delivery of galangin in an aqueous solution for improved antibacterial activity could not be achieved because of its extremely poor water solubility and bioavailbility. The structure and morphology of the resulting hydrogels were verified using with various instrumental techniques using rheometer, FT-IR spectroscopy, solid-state NMR spectroscopy, XRD and FE-SEM. The loading amount of galangin increased as the Cys content in the hydrogels increased, with a release time of 48 h. The galangin loading amount and its cumulative amount released from the Cys/cellulose hydrogel were 1.62- and 1.64-fold greater than those of galangin released from cellulose hydrogel, respectively. Additionally, the galangin-loaded Cys/cellulose hydrogel had antibacterial activity against *S. aureus*, with growth inhibition maintained up to 72 h. Furthermore, the Cys/cellulose hydrogel did not show any cytotoxicity toward human dermal fibroblasts. Throughout the study, the Cys/cellulose hydrogel demonstrated potential advantages as an efficient antibacterial dressing material for galangin delivery through targeting of drugs to the wound site in a sustained manner over a long period without frequent dressing changes.

D. Jeong · H. Kim · J. Jeong · S. Jung
Department of Bioscience and Biotechnology, Microbial Carbohydrate Resource Bank, Konkuk University, 120 Neungdong-ro, Gwangjin-gu, Seoul 05029, South Korea

S. D. Dindulkar · E. Cho · Y.-H. Yang · S. Jung (✉)
Institute for Ubiquitous Information Technology and Applications (UBITA) & Center for Biotechnology Research in UBITA (CBRU), Konkuk University, Seoul 05029, South Korea
e-mail: shjung@konkuk.ac.kr

Y.-H. Yang
Department of Biological Engineering, College of Engineering, Konkuk University, Seoul 05029, South Korea

🌱 Springer

Introduction

Hydrogels have three-dimensional network structures that can hold large amounts of water or other biological fluids (Park et al. 2015) their characteristics depend on the consisting polymers used. These hydrogels have been used for various biomedical, pharmaceutical, and biotechnological applications. Drugs can also easily be encapsulated into the gel for pharmaceutical and biomedical applications. Recently, cellulose-based hydrogels prepared using cross-linking agents have been reported. Cellulose is a biologically safe polymer and the most abundant renewable resource on earth (Kim et al. 2012). The hydroxyl group on cellulose can be modified with various functional groups (Fox et al. 2011), which allows the synthesis of various hydrogels with different properties.

In general, hydrophobic drugs are encapsulated less efficiently into hydrogels than hydrophilic drugs; therefore, a hydrogel cross-linked with β-cyclodextrin (β-CD) was developed to enhance the encapsulation of hydrophobic drugs into the gel (Dong et al. 2014; Pinho et al. 2014). Because the structure of β-CD contains a hydrophilic exterior and hydrophobic cavity, β-CD can form an inclusion complex with hydrophobic compounds in a hydrophilic environment by thermodynamic driving forces, such as hydrogen bonding and van der Waals interactions (Del Valle 2004). However, β-CD has obvious drawbacks as a hydrogel material for drug delivery systems since it has low intrinsic aqueous solubility (18.5 mg/mL at 25 °C), reducing the capacity of hydrogels for water absorption and forming a complex with the drug to inhibit effective release from the gel (Zhang et al. 2013). These binding characteristics of β-CD have been attributed to the rigidity of α-1,4-glycosidic linkages.

Cyclosophoraose (Cys) molecules are unbranched cyclic β-1,2-glucans that are produced by *Rhizobium* species capable of fixing N_2 in association with plants (Abe et al. 1982). Cys is known to play a critical role in nodule formation and induction of crown gall tumors (Geremia et al. 1987). In addition to their physiological functions, Cys possesses encapsulating ability, allowing it to form a complex with hydrophobic molecules, such as some flavonoids, and thus increasing the solubility of guest flavonoids as encapsulating complexes (Lee et al. 2003). Cys also functions as a chiral additive when forming a complex with some chiral molecules, indicating that it has the capacity for chiral recognition during binding (Koizumi et al. 1984; Park et al. 2004). Because the larger cyclic forms are composed of 17–23 glucose units (degree of polymerization: 17–23), Cys and its derivatives (hydroxypropyl Cys or carboxymethyl Cys) are known to form complexes with relatively large hydrophobic guest molecules for biotechnological applications, such as enantioselective separation and solubility enhancement (Jeon et al. 2010; Piao et al. 2014). Since Cys itself is highly water soluble (1350 mg/mL at 25 °C) compared with other well-known cyclo-oligosaccharides, including α-CD, β-CD, and γ-CD, based on the flexible β-1,2-glycosidic linkages and has characteristic encapsulating capacity, Cys-based hydrogels are expected to have the advantages over typical grafted cyclodextrin hydrogels such as high water-swelling capacity, high drug loading capacity and sustained release.

Flavonoids consist of two phenyl rings and a heterocyclic ring and have been used as disease-preventing and health-promoting dietary supplements (Hollman and Katan 1997). Flavonoids can be further divided into five different groups: flavonols, flavones, flavanones, isoflavones, and anthocyanidines. Galangin is a flavonol present in honey and propolis. Galangin has attracted increasing attention owing to its broad pharmacological activities, including antimicrobial, spasmolytic, anti-allergic, anti-inflammatory, anti-viral, and anticarcinogenic activities (Jullian et al. 2010). Recently, galangin has been shown to directly inhibit the activity of β-lactamase and to exhibit intrinsic antibacterial activity (Denny et al. 2002). The inhibition of β-lactamase by galangin has also been shown to enhance the eradication of a strain of methicillin-resistant *Staphylococcus aureus* (*S. aureus*) (Eumkeb et al. 2010). However, both the bioavailability and delivery system of galangin are clearly limited because of its extremely poor water solubility where galangin is sometimes known to be insoluble or hardly soluble (∼14.3 μg/mL) in water and so is miscible in ethanolic water (Cho and Jung 2015; Katyal and Singh 1963; Kim et al. 2014) Although β-CD is known to form a complex with galangin to enhance its aqueous solubility (Jullian et al. 2010), its strong binding capacity and low water-swelling ability could confer intrinsic drawbacks to the use of cyclodextrin-based hydrogels as an efficient delivery system for galangin (Kono et al. 2013).

Herein, we report the preparation of chemically cross-linked Cys/cellulose hydrogels for the efficient delivery of galangin. The structures of the hydrogels were clearly characterized by Fourier transform infrared (FT-IR) spectroscopy, solid-state nuclear magnetic resonance (NMR) spectroscopy, X-ray diffraction (XRD), and field emission scanning electron microscopy (FE-SEM). The swelling and water-retention properties of the Cys/cellulose hydrogels were evaluated. The loading amount and release profile of galangin were also investigated in comparison with other controls. Finally, the galangin-loaded Cys/cellulose hydrogels were evaluated for antibacterial activity against *S. aureus* in a time-dependent manner.

Materials and methods

Materials

Cellulose (microcrystalline, powder, 20 μm), β-CD, and galangin (3,5,7-trihydroxy-2-phenylchromen-4-one) were purchased from Sigma-Aldrich Chemicals Co. (St. Louis, MO, USA). Epichlorohydrin (ECH) was purchased from Daejung Chemical Co., Ltd. (Korea). *S. aureus* ATCC 25923 strains were purchased from the Korean Collection for Type Culture (KCTC, KR).

Purification and characterization of Cys

Precultures of *Rhizobium leguminosarum* biovar viciae VF-39 (*R. leguminosarum* VF-39) were grown in 100-mL Erlenmeyer flasks containing 30 mL of GMS (glutamate mannitol salts) medium on a rotary shaker (200 rpm) at 25 °C for 2 days. The production cultures were carried out in GMS medium with 10 g/L mannitol and 150 mM NaCl (Piao et al. 2014) in 3-L Erlenmeyer flasks containing 1.5 L medium. Higher Cys concentrations were obtained when higher salt concentrations were used in the medium. Production cultures were incubated on a rotary shaker at 25 °C for 14 days. Culture supernatants and microbes were separated by centrifugation at 8000 rpm for 15 min. The culture supernatant was concentrated fivefold using a rotary evaporator. The high-molecular-weight exopolysaccharides were precipitated by adding two volumes of ethanol to the concentrated culture supernatant and

removed by centrifugation at 8000 rpm for 15 min. This supernatant was concentrated fivefold again using a rotary evaporator. Cys-containing low-molecular-weight exopolysaccharides were precipitated by adding another seven volumes of ethanol. The precipitated low-molecular-weight exopolysaccharides were collected by centrifugation at 8000 rpm for 15 min. Cys was purified from these low-molecular-weight exopolysaccharides using three chromatography techniques: size exclusion (Bio-gel P6), anion-exchange (Dowex 1 × 8 chloride form) and desalting (Bio-gel P2). Purified Cys was lyophilized, and the structure of Cys was characterized using matrix-assisted laser desorption ionization time-of-flight mass spectrometry (MALDI-TOF MS; Voyager-DETM STR BioSpectrometry; PerSeptive Biosystems, Framingham, MA, USA) and heteronuclear single quantum coherence (HSQC) NMR (Avance-600; Bruker, Germany) spectroscopic analysis, as shown in our previous reports (Jeong et al. 2012; Piao et al. 2014).

Preparation of hydrogels

Hydrogels were prepared based on previously described methods with some modification (Zhang et al. 2013). Cys (0, 200, or 400 mg) was completely dissolved in 10 mL of NaOH aqueous solution (9 wt%). To each Cys solution, 400 mg cellulose was added. The Cys/cellulose mixture was then stirred for 30 min and stored at −70 °C for 1 h. The frozen mixture was thawed at 25 °C and stirred to obtain a transparent solution in which the cellulose was solubilized completely (Ciolacu et al. 2012). ECH (1 mL) was slowly added to the transparent solution at 25 °C for 1 h to obtain a homogeneous solution, which was then kept at 60 °C for 12 h to prepare the hydrogel. The hydrogels were washed with deionized water (DW) and acetone and stored in a 40 °C vacuum oven for 2 days before being transferred to a freeze dryer (Bondiro; IlShinBioBase, Seoul, Korea). A β-CD/cellulose hydrogel (CD gel) was also prepared using the same process as that used for the Cys gel-2, as described above. The percent hydrogel yield was obtained using the following equation,

$$\text{Hydrogel yield}(\%) = \frac{Dry\ weight\ of\ hydrogel}{Total\ weight\ of\ reactant\ in\ feed\ mixture} \times 100$$

where the total weight of reactant includes the weights of cellulose, Cys, and ECH.

Characterization

Analysis of rheological properties

The rheological properties of hydrogels were evaluated by measuring the storage modulus (G′) and loss modulus (G″) of the swollen hydrogel as a function of angular frequency using an ARES-G2 rheometer (TA Instrument, USA). Experiments were carried out at 25 °C by applying 0.5 % strain between 0.1 and 100 rad/s. The hydrogel samples were prepared as disks and analyzed with a parallel plate measuring 25 mm in diameter, and the gap between plates was adjusted to 3.5 mm.

FT-IR spectroscopy

The FT-IR spectra of Cys, cellulose, Cell gel, and Cys gel-2 were recorded with a Nicolet 6700 FT-IR spectrometer (Thermo Scientific, USA) in the range 4000–500 cm^{-1}. All samples were completely dried and crushed. Potassium bromide pellets were used for all samples.

Solid-state NMR spectroscopy

Dipolar-decoupled/magic angle spinning (DD/MAS) ^{13}C NMR spectra were recorded using a Bruker Biospin AVII 500 spectrometer (BrukerBiospin Co., Ltd., Germany,) with a 4-mm Bruker double resonance broadband MAS probe at a frequency of 10 kHz at 25 °C. The data acquisition time and delay time were set to 50 ms and 20 s, respectively. During the data acquisition period, SPINAL-64 proton decoupling was applied with a 1H field strength of 100 kHz. The spectra were typically accumulated from 3072 scans to achieve an acceptable signal-to-noise ratio.

XRD analysis

The XRD patterns of the dried and crushed samples were recorded on XRD (HR-XRD, D8 Discover; Bruker, USA) with Cu Kα radiation (λ = 0.154 nm). XRD data were collected from $2\theta = 5$–$50°$ at a scanning rate of 1°/min.

FE-SEM

The FE-SEM samples were prepared as follows. The hydrogels were allowed to swell at 25 °C for 24 h and were then frozen in liquid nitrogen and lyophilized. A JSM-6700F (JEOL, Japan) FE-SEM was used to acquire the images of each hydrogel. Double-sided adhesive carbon tape was used to fix the lyophilized samples to a brass stub. The surface of the samples was coated with gold at 30 W for 60 s in a vacuum to render them electrically conductive. The fracture surface of the hydrogels was observed and photographed at an accelerating voltage of 10 kV, 200 × magnification, and working distance (WD) of 8.1 mm.

Swelling characteristic and water-retention properties

All synthesized hydrogels were placed in DW at room temperature for 4 days. Water-swelling degree (Q_1) was calculated using the following equation:

$$Q_n = \frac{W_s - W_d}{W_d} \times 100(\%)$$

where W_s is the weight of the swollen hydrogel, and W_d is the weight of the dried hydrogel. To measure the weight, the hydrogel was removed from the DW, and the remaining water on the surface was gently blotted away with KimWipes (laboratory tissues). The weight was recorded using an analytical balance AUW220D (Shimadzu, Japan), where the scale option was d = 0.01 mg. Water-reswelling degree (Q_2) was determined after drying the hydrogels using the above equation. The water-reswelling ratio was calculated using the following formula:

$$\text{Water reswelling ratio} = \frac{Q_2}{Q_1} \times 100(\%)$$

Water retention was measured as follows. After measuring the weight of dried hydrogels, the samples were placed in DW for 4 days. The water on the surface of the swollen hydrogels was removed, and the gels were placed in an open-mouthed dish at room temperature with a humidity of 25 ± 2 %. Weights were recorded at regular time intervals. The water-retention degree was calculated using the following equation:

$$\text{Water retention degree}(\%) = \frac{W_s - W_d}{W_d} \times 100(\%)$$

In vitro cytotoxicity assay

The cytotoxicity of the hydrogels was evaluated using indirect and direct contact methods (Lin et al. 2013; Pinho et al. 2014). The indirect method was performed as described in ISO 10993-5:2009-Biological evaluation of medical devices, part 5: Tests for in vitro cytotoxicity, by indirect contact. For the cytotoxicity evaluation, human dermal fibroblasts (Seoulin Bioscience, Seoul, Korea) were seeded in 24-well culture plates with an initial density of 3×10^4 per well with high-glucose Dulbecco's modified Eagle medium (DMEM; Hyclone, Logan, UT, USA) containing 10 % fetal bovine serum (FBS) and 1 % penicillin/streptomycin at 37 °C in an atmosphere containing 5 % CO_2. After 24 h, the medium was replaced by hydrogel extracts containing the medium. The hydrogel extracts were prepared as follows. First, 30 mg of hydrogel was immersed in 5 mL of DMEM and then incubated for 18 h at 25 °C in the dark. After incubation for 24 h, 4-(3-[4-iodophenyl]-2-[4-nitrophenyl]-2H-5-tetrazolio)-1.3-benzene disulfonate (WST-1) tests were used for cytotoxicity assessment. To evaluate the cell direct contact cytotoxicity on the hydrogel, Cys, and cellulose, samples (5 mg/mL) were added to 24-well culture plates containing cells at a density of 3×10^4 cells/well for 24 h, respectively. The amount of cell viability was determined using WST-1 assays.

Drug loading and release

Drug loading studies were performed using 1 mg/mL galangin in a solution of DW:ethanol (v/v, 1:1). The dried hydrogels were placed in the above solution at 25 °C for 2 days. After reaching equilibrium, the galangin-loaded hydrogel was washed with DW and then dried completely. The drug-loading capacity was calculated using the following equation:

$$\text{Drug loading capacity} = \frac{(V_1 \times C_1) - (V \times C)}{W_d}$$

where V_1 is the volume of initial drug solution (mL), C_1 is the initial concentration of the drug solution (g/mL), V is the remaining volume of the drug solution (mL), C is the concentration of remaining drug

solution (g/mL), and W_d is the weight of the dry hydrogel (g) (Ciolacu et al. 2012). The concentrations of galangin were determined using a UV–Vis spectrophotometer (UV-2450 spectrophotometer; Shimadzu) at 266 nm. Drug release was observed at 37 °C in phosphate-buffered saline (PBS, pH 7.4) using the dry loaded hydrogel. Aliquots of 0.5 % volume-releasing solution were withdrawn from the PBS periodically. The volume of PBS was held constant by the addition of fresh PBS. The cumulative amount of the drug was calculated as the follows:

Cummulative amount of the drug

$$= C_n V + \sum_{i=1}^{i=n-1} C_i V_i$$

where V is the release media volume, V_i is the sampling volume, C_n and C_i are the drug concentrations in the release media volume and concentration of the extraction samples. The concentrations of drug in PBS were measured in the same manner as for the drug loading studies.

Statistical analyses were carried out with the commercially available SigmaPlot 10.0. The results of drug loading capacity were statistically analyzed with a Student's t test ($p < 0.05$).

Antibacterial activity of galangin-loaded hydrogel

The antibacterial activity of the galangin-loaded hydrogels was assessed against *S. aureus* (a gram-positive bacterium). The galangin-loaded hydrogels (50 mg of dried hydrogel before loading galangin) were incubated in the bacterial suspension (nutrient broth medium, 5 mL, 1.5×10^6 CFU/mL) at 37 °C with 150 rpm in a shaking incubator. A 10-μL aliquot of the bacterial medium was consecutively diluted and then spread onto agar plate (nutrient broth agar plate). After incubation for 24 h, the number of bacteria per milliliter of bacterial culture medium was calculated by multiplying the number of colonies forming unit (CFU) on agar plate by the dilution factor.

Result and discussion

Characterization of Cys

Cys isolated from produced *R. leguminosarum* VF-39 was characterized by MALDI-TOF MS, ^{1}H NMR,

¹³C NMR, and HSQC spectroscopy. These molecules were found to be cyclic glucans composed of 17–23 glucose units based on the MALDI-TOF MS results (Fig. S1 and Table S1). The average molecular weight (M_n) of Cys was 3207 Da and the degree of polymerization was 19. Figure 1 shows the HSQC spectrum of Cys, where ^{13}C and ^{1}H chemical shifts of glucose in Cys were successfully assigned. The correlations at 4.93–4.98 ppm for ^{1}H and at 101.70–102.10 ppm for ^{13}C were assigned, indicating that Cys was solely composed of β-linked glucose residues without any α configuration (York 1995). All chemical shifts of ^{13}C and ^{1}H are listed in Table 1. C2 resonances composed of β-1,2-glycosidic linkages were observed at around 81–82 ppm. The absence of signals at around 92–96 and 73–74 ppm indicated that all C1 and C2 carbons participated in glycosidic bonds (Dell et al. 1983). Taken together, our results showed that Cys was a cyclic β-1,2-glucan with no reducing glucose residues (Jeong et al. 2012).

Table 1 ^{13}C and ^{1}H chemical shift assignments for Cys from *R. leguminosarum* VF-39

C1	101.70–102.10	H1	4.93–4.98
C2	81.71–82.43	H2	3.61–3.66
C3	75.41	H3	3.84
C4	76.30	H4	3.51
C5	68.68	H5	3.55
C6	60.65	H6	3.81
		H6′	3.99

Preparation of hydrogel

Microcrystalline cellulose, having the advantage of high surface area relative to that of native cellulose fibers (Mathew et al. 2005), was used in this study. Kuo et al. demonstrated that 7.1–14.9 wt% NaOH aqueous solution could be optimally designed for the preparation of less than 5 % (w/w) microcrystalline cellulose (Kuo and Hong 2005). Since the optimum

Fig. 1 HSQC spectrum of Cys in D₂O. Blue correlation indicate the proton of CH₂
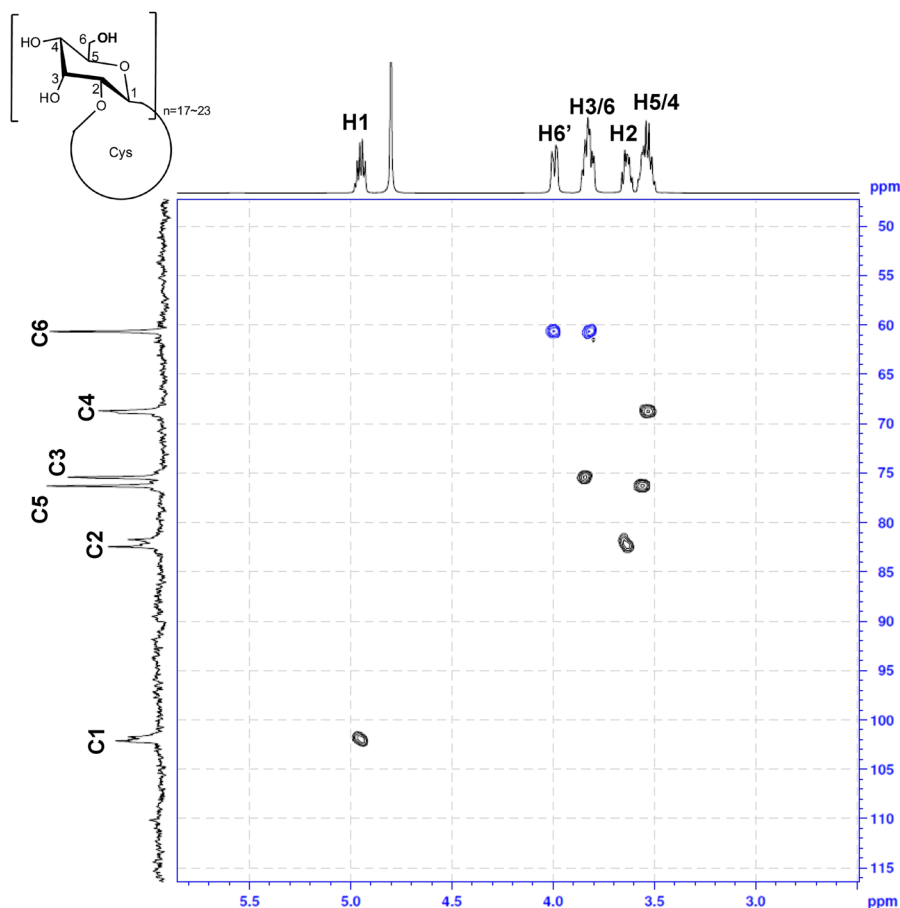
NaOH concentration for the dissolution of microcrystalline cellulose is affected by several factors, including crystalline form, molecular weight, and the amount and degree of crystallinity of the cellulose sample, we investigated the effects of NaOH concentration on the dissolution of 4 % (w/v) microcrystalline cellulose in aqueous solution to prepare the hydrogel. The 4 % (w/v) microcrystalline cellulose in 9 wt% NaOH aqueous solution became transparent after the freeze–thaw process (Fig. S2). Finally, we selected the 9 wt% NaOH aqueous solution for dissolving the microcrystalline cellulose and performed reactions between carbohydrates (Cys and microcrystalline cellulose) and ECH, where ECH was used as a base-catalyzed cross-linking agent that could react with hydroxyl groups of carbohydrates (Scheme 1), as previously reported (Denizli et al. 2004). In this study, three types of Cys/cellulose hydrogels were prepared as following: Cell gel with 4 % (w/v) cellulose; Cys gel-1 with 2 % (w/v) Cys and 4 % (w/v) cellulose; and Cys gel-2 with 4 % (w/v) Cys and 4 % (w/v) cellulose. As a control, β-CD/cellulose hydrogel (CD gel) was also prepared using 4 % (w/v) β-CD and 4 % (w/v) cellulose. The hydrogel yields of Cell gel, Cys gel-1, Cys gel-2, and CD gel were 30, 34, 35, and 35 %, respectively. All hydrogel yields were similar, despite the increase in Cys concentration in the feed mixture, indicating induction of effective cross-linking of Cys with cellulose.

Hydrogel characterization

Figure 2 shows images of Cell gel and Cys gel-2. The high Cys content in Cys gel-2 (Fig. 2d) results in a relatively low transparency compared with that of the Cell gel (Fig. 2b). Since translucent cellulose-based gels have been shown to have higher mechanical strength (Chang et al. 2010), we assumed that Cys and cellulose were effectively packed, with higher mechanical strength in Cys gel-2. We also evaluated the rheological properties of each swollen hydrogel using a rheometer (Fig. 3). When all the hydrogels form a well-structured network, the storage modulus (G′) values of hydrogels are always higher than loss modulus (G″) values (Siemoneit et al. 2006). As shown in Fig. 3, the G′ value increased according to the increase in Cys concentration in the hydrogels. The Cys gel-2 showed the highest storage modulus among hydrogels. Additionally, the higher feed amount of

Cys improved the mechanical strength of the hydrogel. These results clearly indicated that Cys gel-2 had a more compact network structure than the other hydrogels.

FT-IR spectroscopy analysis

Figure 4 shows the FT-IR spectra of Cys, cellulose, Cell gel, and Cys gel-2. The presented bands in the Cys spectrum at 3372, 2886, 1020, and 892 cm^{-1} were assigned to the stretching of –OH groups, C–H stretching, C–O–C pyranose ring skeletal vibration, and glycosidic C_1–H deformation with ring vibration contribution, respectively. The characteristic bands of cellulose largely overlapped with those of Cys, but shifted due to the different glycosidic linkages composed of common β-D-glucose units (Fig. 4a). In the Cell gel spectrum, the O–H stretching band was shifted from 3334 to 3373 cm^{-1} compared with that of cellulose. This change is consistent with the results of typical cellulose hydrogels prepared using ECH as a cross-linking agent (Zhang et al. 2013). The characteristic absorption band of the epoxy ring at 1260 cm^{-1} and the peaks of C–Cl stretching at 721 cm^{-1} disappeared. In contrast, both the absorption bands of O–H stretching and C–O–C pyranose ring vibration in Cys gel-2 were decreased due to the new ether bonds formed by the cross-linking reactions, which generally cause C–O–C peaks to be weaker and wider, as shown in Fig. 4b. This indicated that the cross-linking reaction between cellulose and Cys by ECH successfully occurred in the NaOH solution, suggesting that the residual binary functional group of ECH was absent in the hydrogels (Gao and Zhao 2004; Lin and Dufresne 2013).

Solid-state NMR analysis

The chemical structure of insoluble amorphous hydrogel was investigated by ^{13}C solid state NMR (Chang et al. 2010). Figure 5 shows the solid-state DD/MAS ^{13}C NMR spectra of the cellulose, Cys, and hydrogels. All observed chemical shifts are listed in Table S2. In the ^{13}C NMR spectra, C1, C4, and C6 peaks of the anhydroglucose unit in cellulose appeared at 104.99, 83.80, and 63.43 ppm, respectively, and the C2, C3, and C5 peaks overlapped at around 73.96 ppm. In the ^{13}C NMR spectrum of Cys, C1′, C4′, and C6′ carbon peaks appeared at
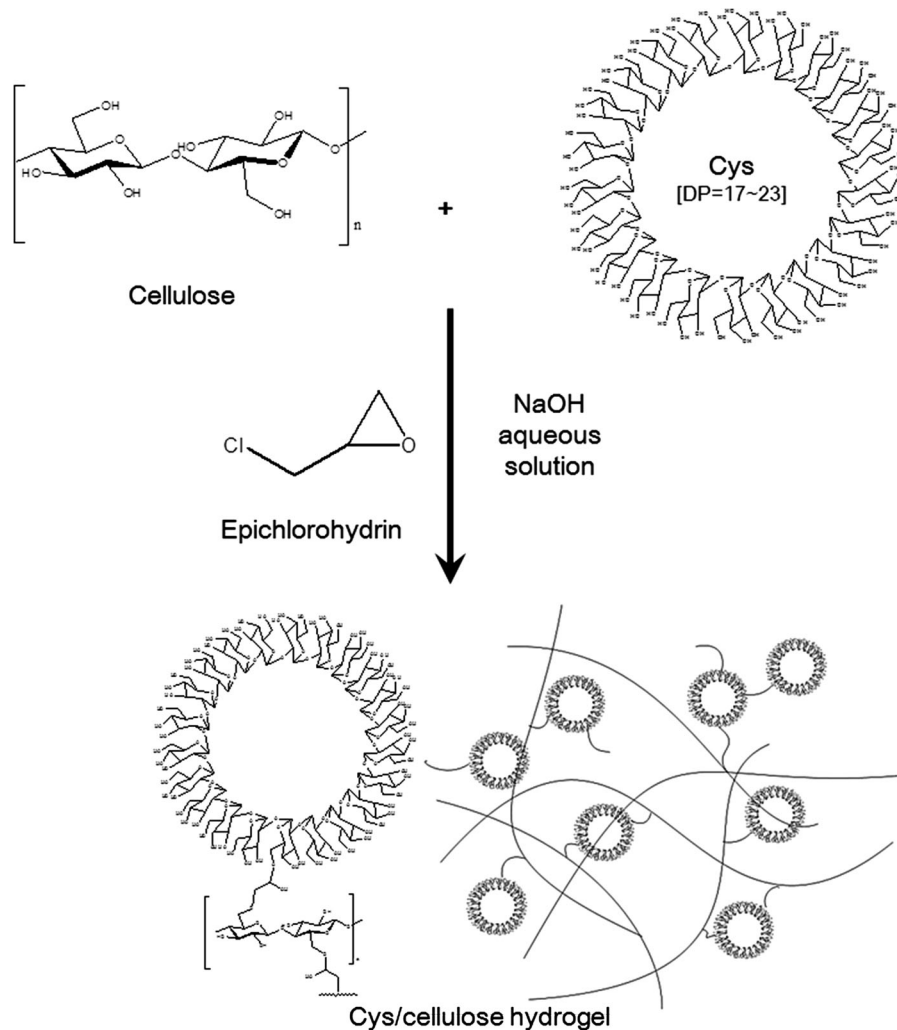
Scheme 1 Scheme for the Cys/cellulose hydrogel

104.42–101.84, 70.24, and 62.64 ppm, respectively, and the C2′, C3′, and C5′ peaks overlapped at around 76.65 ppm. Broad peaks from 101 to 104 ppm around C1′ of the anhydroglucose residue in Cys were characteristic due to the flexible β-1,2-glycosidic linkage of Cys (York 1995). In contrast, cellulose containing a β-1,4-glycosidic linkage showed a characteristic C1 peak at around 104 ppm in both cellulose and cellulose gel. As shown in Fig. 5, Cys gel-1/2 showed new peaks at around 101.75 ppm as Cys was incorporated into the cellulose gel after normalization of the spectra according to the peak intensity of the C1 carbon (Fig. 5b). The other C peaks of anhydroglucose units

in Cys gel-2 showed a characteristic downfield shift after the crosslinking reaction with Cys, in which the peaks at around 73.9 and 63.9 ppm, corresponding to C2–C6 carbons, shifted downfield to 74.4 and 64.4 ppm, respectively, after the formation of Cys gel-2. Although we could not clearly normalize the ¹³C NMR spectrum for calculation of the degree of cross-linking of Cys onto cellulose owing to the lack of characteristic peaks for normalization between Cys and cellulose, the difference in the glycosidic linkage could provide clear evidence of cross-linking between Cys and cellulose throughout analysis of C1 peaks of anhydroglucose units of the hydrogels in the solid-state ¹³C NMR spectra (Fig. 5b).
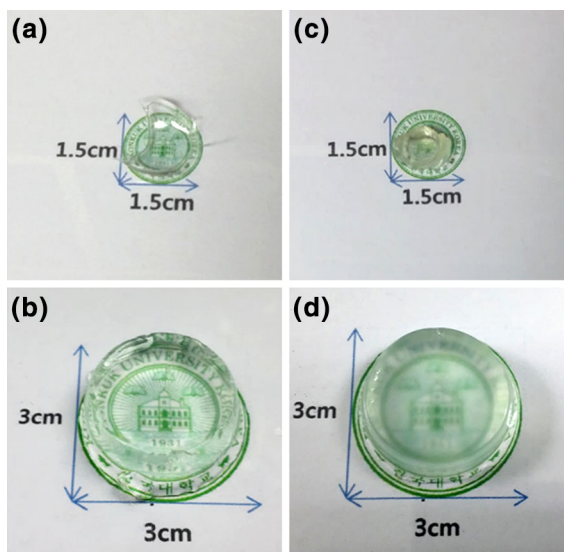
Fig. 2 Photographs of Cell gel (**a**, **b**), Cys gel-2 (**c**, **d**). Dry hydrogels (**a**, **c**), hydrogels after incubation in DW for 4 days (**b**, **d**)
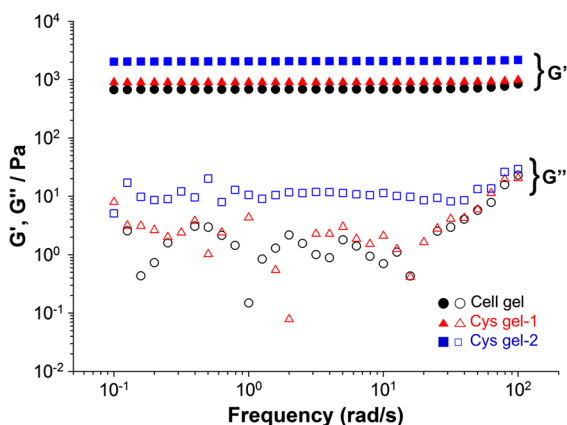
Fig. 3 The frequency dependence of storage modulus (G′) and loss modulus (G″) for the hydrogels

XRD analysis

XRD patterns of Cys, cellulose, Cell gel, Cys gel-1, and Cys gel-2 are presented in Fig. 6. XRD patterns did not reveal any diffraction peaks with strong intensity in Cys; only two smooth peaks were observed at 10° and 15°–25° (Fig. 6a), a pattern assigned to amorphous structures. The microcrystalline form of cellulose exhibited diffraction peaks at 2θ around 15°, 22°, and 35° (Fig. 6b). This pattern is comparable to the XRD pattern of cellulose in

crystalline form (Isogai et al. 1989). After the formation of the hydrogel, the entire diffraction peak from Cys and cellulose disappeared, and only one broad peak appeared at 17°–19°. As the Cys concentration increased, the intensity of the peak at 17°–19° decreased slightly, suggesting that the chemical crosslinking among the cellulose, Cys, and ECH changed the XRD pattern of the crystallization of cellulose and Cys and increased the amorphous region in the hydrogels.

FE-SEM analysis

Figure 7 shows the FE-SEM images of the cross-section of swollen hydrogels after a 4 day incubation period. The Cell gel exhibited a complex network and irregular pore size and distribution. In contrast to the Cell gel, the increase in Cys concentration in the Cys gel-2 increased the pore size and distribution even more, suggesting that inserting Cys into the gel formation affected these two factors. From the plot profiles of the selected 400-µm line in the SEM image according to the Fiji image processing package (Cho et al. 2015), various irregular gap widths of the pore were observed in the Cell gel (Fig. 7d); however, relatively regular gap widths were found in the Cys gel-2 (Fig. 7f).

Water swelling and water retention degree

High swelling degrees in the hydrogels have many advantages in biomedical applications, such as quick hemostatic ability and preventing the wound bed from accumulation of exudates (Li et al. 2011). The water-swelling degrees (Q_1) of the hydrogels for Cell gel, Cys gel-1, Cys gel-2 and CD gel were found to be 5773, 5048, 4877, and 4707, respectively (Fig. 8a). In the case of the water-swelling profile for the hydrogels (Fig. 8b), the relaxation rate of water swelling for all hydrogels was found to be similar at equilibrium (72 h), likely owing to the similar network structure since all the hydrogels were prepared using the same concentrations of cellulose and ECH.
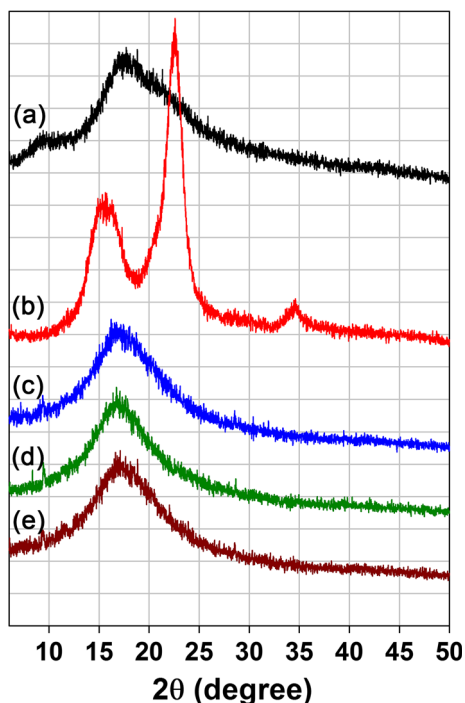
However, the water-reswelling degrees (Q_2) of the hydrogels compared with the Q_1 values differed substantially depending on the components of the hydrogels (Fig. 8a). The ratios of water-reswelling for the Cell gel, Cys gel-1, Cys gel-2, and CD gel were 82, 77, 82, and 70 %, respectively, indicating that Cys gel-
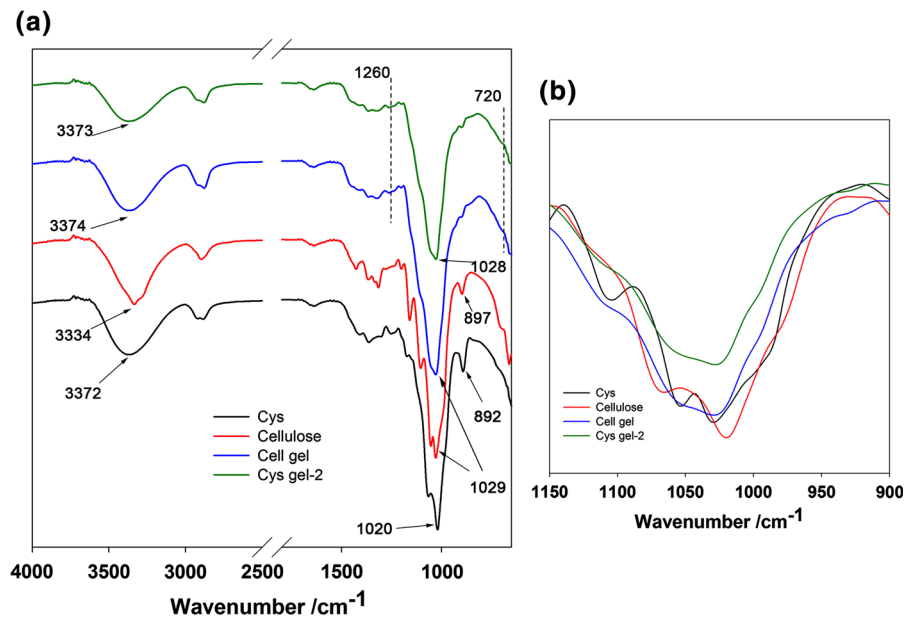
Fig. 4 **a** FT-IR spectra of Cys, cellulose, Cell gel, and Cys gel-2. **b** The partial FT-IR spectra of Cys, cellulose, Cell gel, and Cys gel-2

Fig. 5 **a** Solid-state DD/MAS ^{13}C NMR spectra of the cellulose, Cys and hydrogels. **b** The partial solid-state DD/MAS ^{13}C NMR spectra of the cellulose, Cys and hydrogels. These spectra were normalized by peak intensity of the C1 carbon
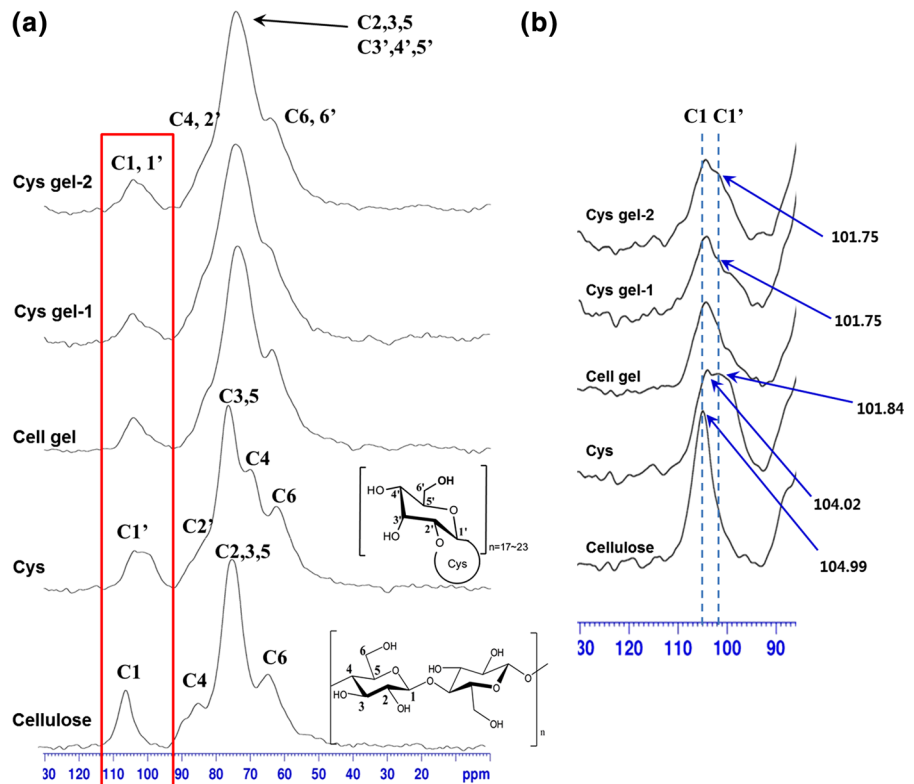
Fig. 6 XRD patterns of **a** Cys, **b** cellulose, **c** Cell gel, **d** Cys gel-1 and **e** Cys gel-2

2 had a water-reswelling ratio similar to that of the Cell gel. However, the water-reswelling ratio of the Cys gel-2 was much higher than that of the CD gel. This difference could be explained by differences in the characteristics of the physiochemical structures between Cys and CD. Figure 8c shows the water-retention degree profiles of the Cell gel, Cys gel-1, Cys gel-2, and CD gel from 0 to 57 h. The Cys gel-1/2 showed a pattern similar to that of the Cell gel, whereas the Cys gel exhibited a higher water-retention degree than the CD gel during the 60 h test period. The CD gel became completely dry after 45 h. The decreased water concentration inside of the CD gel may increase the hydrophobic region and disrupt bonding between hydrogen and water (Kono et al. 2013).

In previous studies, CD gel was used as a delivery system for some hydrophobic drugs, despite its relatively poor water-swelling capacity and water retention degree. The β-CD within the hydrogel may provide advantages to the hydrogels because β-CD can capture the target drug by inclusion complexation (Machín et al. 2012). In our analysis, we confirmed that the Cys/cellulose hydrogel exhibited better

potential as a delivery system than did the β-CD/cellulose hydrogel because each of the water-swelling capacity and water retention time in Cys/cellulose hydrogel was 581 % higher and 10 h longer than β-CD/cellulose hydrogel, respectively.

In vitro cytotoxicity assay

The in vitro cell cytotoxicity of hydrogels was evaluated by the indirect and direct contact methods. The results of indirect contact cytotoxicity assays are shown in Fig. 9a. Compared with control, cell viability of Cell gel, Cys gel-1 and Cys gel-2 extracts was 97, 99 and 96 %, respectively. Extracts of all hydrogels did not have substantial effects on the viability of human dermal fibroblasts. In the case of the direct contact study (Fig. 9b), there were no differences in cell viability compared with that in the control. Cys and cellulose also did not show any cytotoxic effects on human dermal fibroblasts. These results indicate that Cys gel-1 and Cys gel-2 may have promise as medical dressing materials without inducing any skin damage.

Galangin loading and release

Because host–guest complexation technology can be used to enhance the aqueous solubility of drugs that exhibit poor water solubility (Cho and Jung 2015; Jullian et al. 2010), we prepared the Cys/cellulose hydrogels as an efficient delivery system for poorly soluble galangin. For efficient galangin loading to the hydrogels, an aqueous ethanol-based solution (ethanol:water, 1:1) was used, as described previously (Watanabe et al. 2013). The average loading capacities of galangin in Cell gel, Cys gel-1, Cys gel-2, and CD gel were 10.96, 14.66, 17.77, and 18.8 mg/g dry hydrogel, respectively (Fig. 10). Each of the observed difference for galangin loading capacity of Cys gel-1 ($p = 0.01$), Cys gel-2 ($p = 0.002$) and CD gel ($p = 0.006$) was statistically significant compared with the cellulose gel on the basis of Student's t test ($p < 0.05$). The maximum drug loading of the CD gel was partially overlapped that of Cys gel-2, likely due to the molecular complexation of β-CD or Cys with galangin.

Figure 11 shows the in vitro release profiles of galangin in PBS (pH 7.4). PBS provides pseudophysiological conditions and is commonly used for
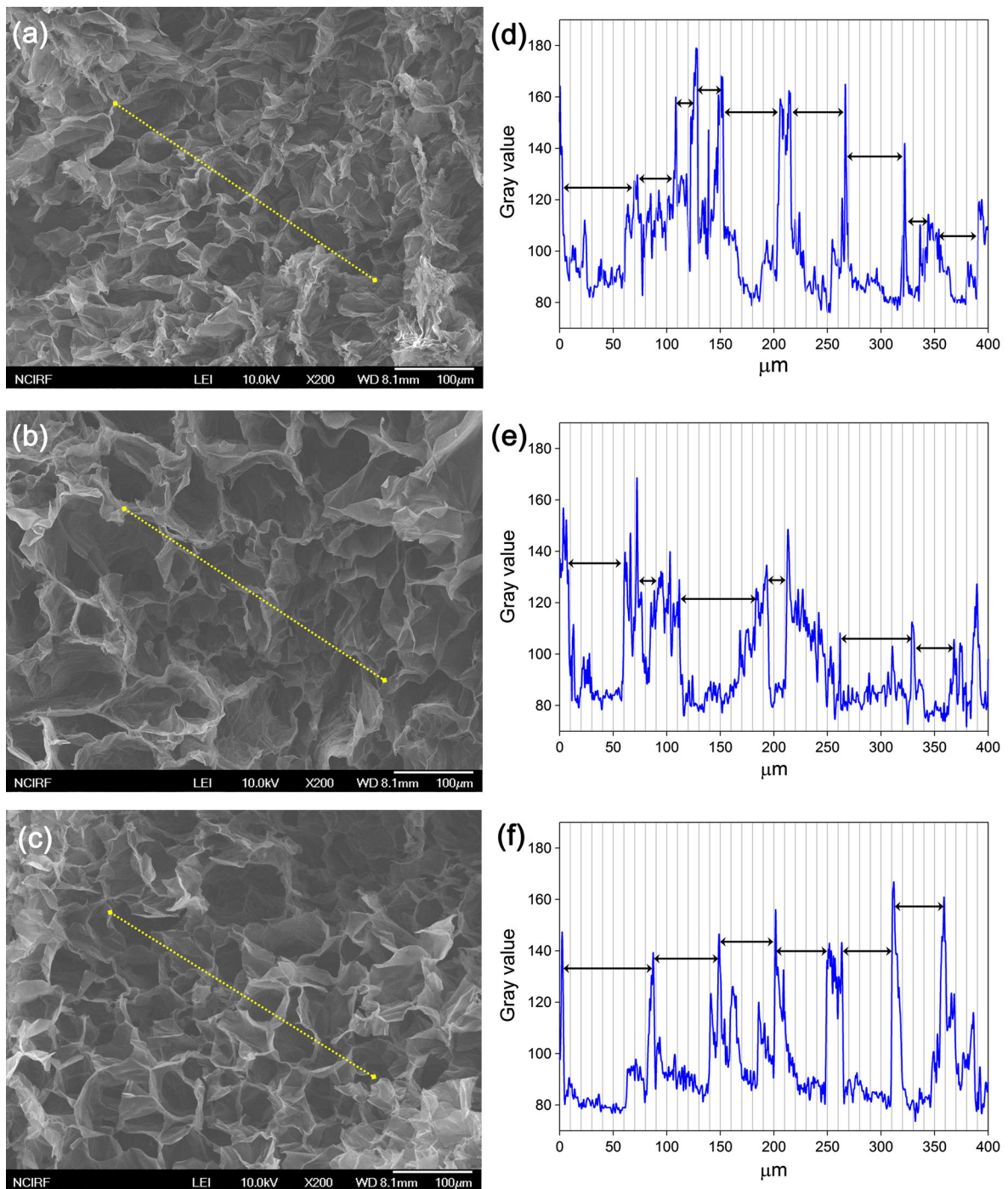
Fig. 7 FE-SEM images of the hydrogels: **a** Cell gel, **b** Cys gel-1 and **c** Cys gel-2. Plot profiles of the selected yellow line of **d** Cell gel, **e** Cys gel-1 and **f** Cys gel-2. *Black arrows* indicate the gap width

evaluation of drug release (Constantin et al. 2014). The galangin-release profiles of all the hydrogels exhibited burst release during the first 5 h. This

increase was ascribed to the rapid dissolution of galangin from the surface of hydrogels before diffusing into the solution. The release was sustained after
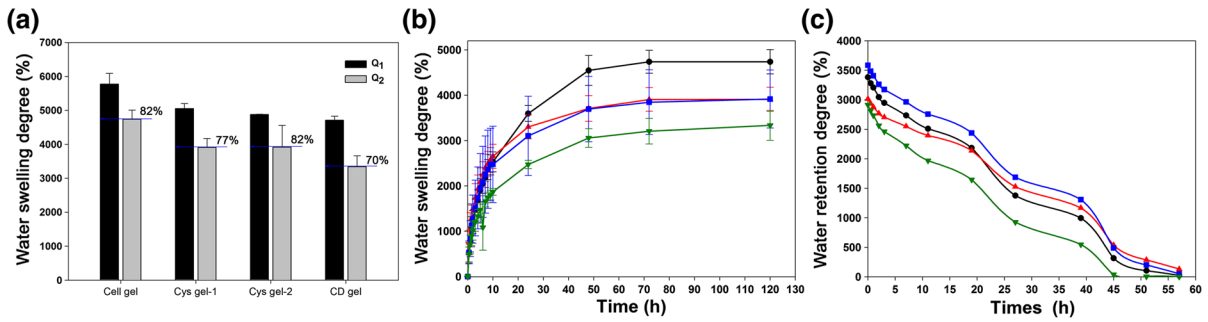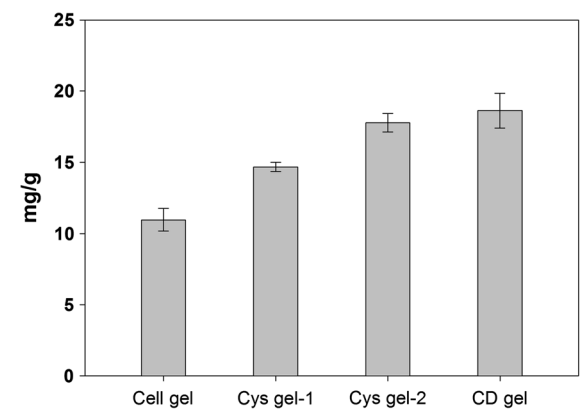
Fig. 8 a Water-swelling and water-reswelling degree of Cell gel, Cys gel-1, Cys gel-2, and CD gel. b Water-swelling degree profiles in DW of Cell gel (*filled circle*), Cys gel-1 (*filled triangle*), Cys gel-2 (*filled square*), and CD gel (*filled inverted triangle*). c Water-retention degree profiles of Cell gel (*filled circle*), Cys gel-1 (*filled triangle*), Cys gel-2 (*filled square*), and CD gel (*filled inverted triangle*) at room temperature, 25 ± 2 % humidity
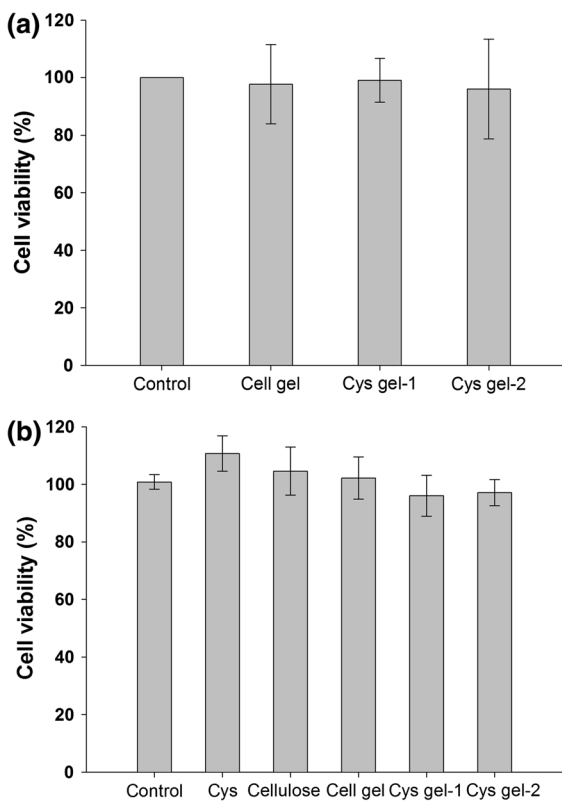
Fig. 9 a Indirect cytotoxicity of the extracts from hydrogels. b Direct contact cytotoxicity of materials and hydrogels

Fig. 10 Galangin loading amounts in Cell gel, Cys gel-1, and Cys gel-2. Loading was performed for 48 h at 25 °C with galangin dissolved in 5:5 DW:ethanol (v/v)

5 h owing to the diffusion of galangin from the microporous matrix in the hydrogel as swelling continued. The equilibrium times of galangin release in Cell gel, Cys gel-1, Cys gel-2, and CD gel were approximately 24, 24, 48, and 48 h, respectively. 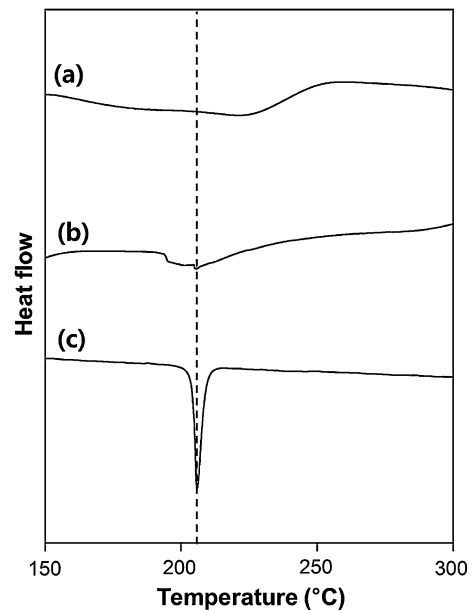The galangin release behaviors were relatively similar for all hydrogels. However, the maximum amount of galangin release at equilibrium was observed for the Cys gel-2, and the release order was as follows: Cys gel-2 > Cys gel-1 > CD gel > Cell gel. As shown in Fig. 11b, effective galangin release was observed in Cys gels compared with that of Cell gel or CD gel. The lowest galangin release was observed for the CD gel, even though the amount of galangin loaded in the hydrogel was the highest for the CD gel. This may be explained by the strong binding ability of CD to galangin and the low water-swelling capacity of the α-1,4-glycosidic linkage of CD (Zhang et al. 2013). The Cys gel-2, however, exhibited effective galangin release due to the flexible molecular conformation of the β-1,2-glycosidic linkage of Cys in the Cys gel-2 (Choi et al. 2000). This efficient galangin release could be ascribed to the direct complexation of galangin with

(a)

(b)
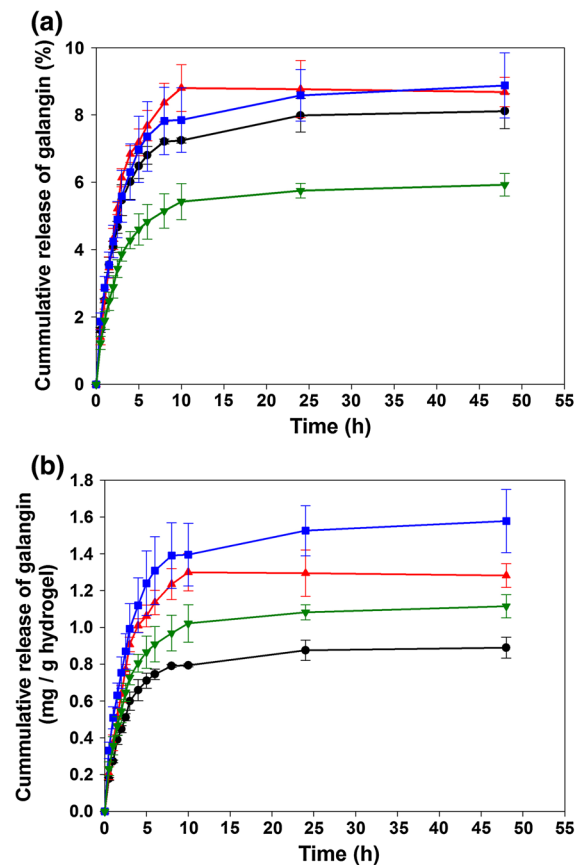
Fig. 11 Galangin-releasing profiles of Cell gel (*filled circle*), Cys gel-1 (*filled triangle*), Cys gel-2 (*filled square*), and CD gel (*filled inverted triangle*). **a** Cumulative percentage of galangin released. **b** Cumulative amount of galangin (mg) released per amount of hydrogel (g). Profiles were performed for 48 h at 37 °C with PBS buffer (pH 7.4)

Fig. 12 DSC curves of galangin loaded **a** Cys gel-2, **b** galangin loaded Cell gel and **c** galangin

Cys inside of the Cys gel-2. Thus, we investigated the direct complexation of Cys with galangin using differential scanning calorimetry (DSC) analysis (Fig. 12). The sharp endothermic peak of galangin only (Fig. 12c) appeared at 210 °C at its melting point. In the galangin-loaded Cell gel (Fig. 12b), the galangin endothermic peak was decreased but still present. However, for the galangin-loaded Cys gel-2, the endothermic peak of galangin disappeared completely (Fig. 12a), indicating that the galangin molecules directly interacted with the Cys inside of the Cys gel-2 through various molecular interactions, including hydrogen bonds or van der Waals interactions (Machín et al. 2012). These results indicated that the Cys gel could effectively release galangin by

formation of a molecular complex with Cys inside of the hydrogels.

Antibacterial activities of hydrogels loaded with galangin

Staphylococcus aureus is an important human pathogen that causes a variety of diseases, including pneumonia, septicemia, endocarditis, and osteomyelitis (Pan et al. 2002). Galangin possesses antibacterial activity and results in a 1000-fold reduction in viable counts of *S. aureus* (Cushnie et al. 2003). This antibacterial activity was investigated in galangin-loaded hydrogels by assessing the growth-inhibitory effects of the hydrogels using CFU counting (Fig. 12a). The lag, log, stationary, and death phases of untreated bacterial suspensions were defined as the time periods from 0 to 4, 4 to 18, 18 to 42, and 42 to 72 h, respectively. No antibacterial activities were observed in both Cys and cellulose alone, indicating that these biomaterials did not affect the growth of *S. aureus* (Fig. S3). However, galangin-loaded hydrogels inhibited bacterial growth during the lag phase. Galangin was released rapidly from the hydrogel surfaces during this lag phase, resulting in significant antibacterial activity against *S. aureus*. Bacterial
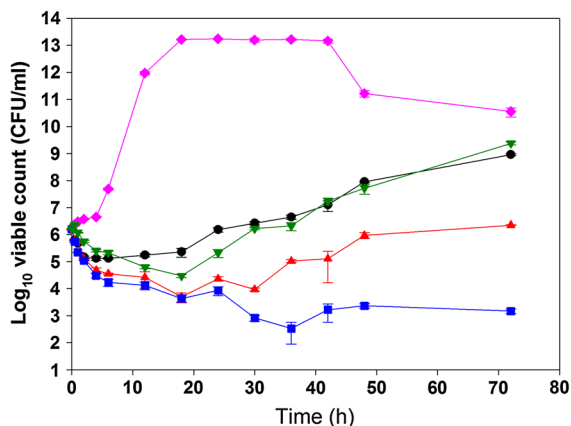
Fig. 13 Antibacterial activity of galangin-loaded Cell gel (*filled circle*), Cys gel-1 (*filled triangle*), Cys gel-2 (*filled square*), and CD gel (*filled inverted triangle*) against viable counts of *S. aureus*. The control was galangin-untreated *S. aureus* (*filled diamond*). Galangin-loaded hydrogels (50 mg) were placed in a *S. aureus* suspension medium (nutrient broth medium, 5 ml, 1.5×10^6 CFU/ml) at 37 °C with 150 rpm in a shaking incubator

growth inhibition by all galangin-loaded hydrogels continued to the log phases, indicating that the antibacterial activity of the galangin-loaded hydrogels was maintained during the log phase. However, normal bacterial growth was again observed in Cell gel, Cys gel-1, and CD gel after 18 h. In particular, the results from the Cys gel-2 were significantly different from those of the other gels, particularly in terms of viable cell count after 72 h of incubation. The viable cell count in the Cell gel, Cys gel-1, and CD gel increased up to 10^9, 10^6, and 10^9, respectively, while that of the Cys gel-2 remained at 10^3, demonstrating remarkable antibacterial activity. In the case of Cys gel-2, the percentage of antibacterial activity reached up to 99.99999 % for 72 h, whereas those of Cell gel and CD gel showed 97.60 and 93.27 % (Fig. S4). These results indicated that the Cys/cellulose hydrogel had the potential to act as an efficient galangin release system, and therefore, could be used to prevent bacterial infection in wounds (Fig. 13).

Conclusions

Cys/cellulose hydrogels were successfully prepared by cross-linking Cys and cellulose. Various properties, such as the water absorbability, water-retention ratio, galangin-loading amount, and release pattern, were

then investigated for the prepared hydrogels. The results were compared with those of cellulose hydrogel and β-CD/cellulose hydrogel, which were used as controls. The water reswelling degree and water retention profiles of Cys/cellulose hydrogel were similar to those of the cellulose hydrogel, indicating that Cys was so hydrophilic that it did not influence the water absorption properties of the cellulose hydrogel. The Cys/cellulose hydrogel outperformed the cellulose and CD/cellulose hydrogel as a galangin delivery system in terms of loading amount and sustainable release of galangin, where galangin was encapsulated into the Cys/cellulose hydrogel network, allowing sustained, robust release for 48 h. Furthermore, the galangin-loaded Cys/cellulose hydrogel exhibited excellent antibacterial activity after long incubation periods (72 h) with *S. aureus*. In our current study, the Cys/cellulose hydrogel exhibited potential advantages for application as an efficient galangin delivery system, including the relatively high water-swelling degree, long water retention time, and effective drug release pattern. The Cys/cellulose hydrogel may have the potential to provide a method for delivering poorly water-soluble drugs to the wound site in a sustained manner over a long time without the requirement for frequent dressing changes.

References

Abe M, Amemura A, Higashi S (1982) Studies on cyclic β-1,2-glucan obtained from periplasmic space of *Rhizobium trifolii* cells. Plant Soil 64:315–324. doi:10.1007/bf02372514

Chang C, Zhang L, Zhou J, Zhang L, Kennedy JF (2010) Structure and properties of hydrogels prepared from cellulose in NaOH/urea aqueous solutions. Carbohydr Polym 82:122–127. doi:10.1016/j.carbpol.2010.04.033

Cho E, Jung S (2015) Supramolecular complexation of carbohydrates for the bioavailability enhancement of poorly soluble drugs. Molecules 20:19620–19646

Cho E, Tahir MN, Kim H, Yu J-H, Jung S (2015) Removal of methyl violet dye by adsorption onto N-benzyltriazole derivatized dextran. RSC Adv 5:34327–34334

Choi Y-H, Yang C-H, Kim H-W, Jung S (2000) Molecular dynamics simulations of cyclohenicosakis-[(1 → 2)-β-d-gluco-henicosapyranosyl], a cyclic (1 → 2)-β-D-glucan (a 'cyclosophoraose') of DP 21. Carbohydr Res 326:227–234. doi:10.1016/S0008-6215(00)00050-1

Ciolacu D, Oprea AM, Anghel N, Cazacu G, Cazacu M (2012) New cellulose–lignin hydrogels and their application in

controlled release of polyphenols. Mater Sci Eng, C 32:452–463. doi:10.1016/j.msec.2011.11.018

Constantin M, Bucatariu S, Harabagiu V, Ascenzi P, Fundueanu G (2014) Do cyclodextrins bound to dextran microspheres act as sustained delivery systems of drugs? Int J Pharm 469:1–9

Cushnie TT, Hamilton VE, Lamb AJ (2003) Assessment of the antibacterial activity of selected flavonoids and consideration of discrepancies between previous reports. Microbiol Res 158:281–289

Del Valle EMM (2004) Cyclodextrins and their uses: a review. Process Biochem 39:1033–1046. doi:10.1016/S0032-9592(03)00258-9

Dell A, York WS, McNeil M, Darvill AG, Albersheim P (1983) The cyclic structure of β-D-(1 → 2)-linked D-glucans secreted by Rhizobia and Agrobacteria. Carbohydr Res 117:185–200

Denizli BK, Can HK, Rzaev ZMO, Guner A (2004) Preparation conditions and swelling equilibria of dextran hydrogels prepared by some crosslinking agents. Polymer 45:6431–6435. doi:10.1016/j.polymer.2004.07.067

Denny BJ, Lambert PA, West PW (2002) The flavonoid galangin inhibits the L1 metallo-β-lactamase from Stenotrophomonas maltophilia. FEMS Microbiol Lett 208:21–24

Dong C, Qian L-Y, Zhao G-L, He B-H, Xiao H-N (2014) Preparation of antimicrobial cellulose fibers by grafting β-cyclodextrin and inclusion with antibiotics. Mater Lett 124:181–183. doi:10.1016/j.matlet.2014.03.091

Eumkeb G, Sakdarat S, Siriwong S (2010) Reversing β-lactam antibiotic resistance of Staphylococcus aureus with galangin from Alpinia officinarum Hance and synergism with ceftazidime. Phytomedicine 18:40–45

Fox SC, Li B, Xu D, Edgar KJ (2011) Regioselective esterification and etherification of cellulose: a review. Biomacromolecules 12:1956–1972

Gao Z, Zhao X (2004) Preparation and electrorheological characteristics of β-cyclodextrin–epichlorohydrin–starch polymer suspensions. J Appl Polym Sci 93:1681–1686

Geremia RA, Cavaignac S, Zorreguieta A, Toro N, Olivares J, Ugalde RA (1987) A Rhizobium meliloti mutant that forms ineffective pseudonodules in alfalfa produces exopolysaccharide but fails to form beta-(1–2) glucan. J Bacteriol 169:880–884

Hollman P, Katan M (1997) Absorption, metabolism and health effects of dietary flavonoids in man. Biomed Pharmacother 51:305–310

Isogai A, Usuda M, Kato T, Uryu T, Atalla RH (1989) Solid-state CP/MAS carbon-13 NMR study of cellulose polymorphs. Macromolecules 22:3168–3172

Jeon Y, Kwon C, Cho E, Jung S (2010) Carboxymethylated cyclosophoraose as a novel chiral additive for the stereoisomeric separation of some flavonoids by capillary electrophoresis. Carbohydr Res 345:2408–2412. doi:10.1016/j.carres.2010.08.009

Jeong D, Piao J, Kwon C, Jung S (2012) Synthesis of oligomeric microbial cyclosophoraoses as novel complexation agents. Bull Korean Chem Soc 33:2095–2098

Jullian C, Alfaro M, Zapata-Torres G, Olea-Azar C (2010) Inclusion complexes of cyclodextrins with galangin: a

thermodynamic and reactivity study. J Solut Chem 39:1168–1177. doi:10.1007/s10953-010-9574-1

Katyal M, Singh R (1963) Spectrophotometric determination of zirconium and other colour reactions by galangin. In: Proceedings of the Indian Academy of Sciences-Section A, 1963, vol 4. Springer, pp 259–265

Kim MH, An S, Won K, Kim HJ, Lee SH (2012) Entrapment of enzymes into cellulose–biopolymer composite hydrogel beads using biocompatible ionic liquid. J Mol Catal B: Enzym 75:68–72. doi:10.1016/j.molcatb.2011.11.011

Kim H, Choi J, Choi Y, Tahir M, Yang Y-H, Cho E, Jung S (2014) Enhanced solubility of galangin based on the complexation with methylated microbial cyclosophoraoses. J Incl Phenom Macrocycl Chem 79:291–300. doi:10.1007/s10847-013-0351-9

Koizumi K, Okada Y, Horiyama S, Utamura T, Higashiura T, Ikeda M (1984) Preparation of cyclosophoraose-A and its complex-forming ability. J Incl Phenom 2:891–899. doi:10.1007/bf00662259

Kono H, Onishi K, Nakamura T (2013) Characterization and bisphenol A adsorption capacity of β-cyclodextrin–carboxymethylcellulose-based hydrogels. Carbohydr Polym 98:784–792. doi:10.1016/j.carbpol.2013.06ki.065

Kuo YN, Hong J (2005) Investigation of solubility of microcrystalline cellulose in aqueous NaOH. Polym Adv Technol 16:425–428

Lee S, D-h Seo, H-l Park, Choi Y, Jung S (2003) Solubility enhancement of a hydrophobic flavonoid, luteolin by the complexation with cyclosophoraoses isolated from Rhizobium meliloti. Antonie Van Leeuwenhoek 84:201–207

Li H, Yang J, Hu X, Liang J, Fan Y, Zhang X (2011) Superabsorbent polysaccharide hydrogels based on pullulan derivate as antibacterial release wound dressing. J Biomed Mater Res A 98:31–39

Lin N, Dufresne A (2013) Supramolecular hydrogels from in situ host–guest inclusion between chemically modified cellulose nanocrystals and cyclodextrin. Biomacromolecules 14:871–880

Lin W-C, Lien C-C, Yeh H-J, Yu C-M, S-h Hsu (2013) Bacterial cellulose and bacterial cellulose–chitosan membranes for wound dressing applications. Carbohydr Polym 94:603–611

Machín R, Isasi JR, Vélaz I (2012) β-Cyclodextrin hydrogels as potential drug delivery systems. Carbohydr Polym 87:2024–2030

Mathew AP, Oksman K, Sain M (2005) Mechanical properties of biodegradable composites from poly lactic acid (PLA) and microcrystalline cellulose (MCC). J Appl Polym Sci 97:2014–2025

Pan X-S, Hamlyn PJ, Talens-Visconti R, Alovero FL, Manzo RH, Fisher LM (2002) Small-colony mutants of Staphylococcus aureus allow selection of gyrase-mediated resistance to dual-target fluoroquinolones. Antimicrob Agents Chemother 46:2498–2506

Park H, Lee S, Kang S, Jung Y, Jung S (2004) Enantioseparation using sulfated cyclosophoraoses as a novel chiral additive in capillary electrophoresis. Electrophoresis 25:2671–2674. doi:10.1002/elps.200405971

Park S et al (2015) Application of cellulose/lignin hydrogel beads as novel supports for immobilizing lipase. J Mol

Catal B: Enzym 119:33–39. doi:10.1016/j.molcatb.2015.05.014

Piao J et al (2014) Solubility enhancement of α-naphthoflavone by synthesized hydroxypropyl cyclic-(1 → 2)-β-d-glucans (cyclosophoroases). Carbohydr Polym 101:733–740

Pinho E, Henriques M, Soares G (2014) Cyclodextrin/cellulose hydrogel with gallic acid to prevent wound infection. Cellulose 21:4519–4530. doi:10.1007/s10570-014-0439-4

Siemoneit U, Schmitt C, Alvarez-Lorenzo C, Luzardo A, Otero-Espinar F, Concheiro A, Blanco-Méndez J (2006) Acrylic/cyclodextrin hydrogels with enhanced drug loading and sustained release capability. Int J Pharm 312:66–74. doi:10.1016/j.ijpharm.2005.12.046

Watanabe K, Nishio Y, Makiura R, Nakahira A, Kojima C (2013) Paclitaxel-loaded hydroxyapatite/collagen hybrid gels as drug delivery systems for metastatic cancer cells. Int J Pharm 446:81–86

York WS (1995) A conformational model for cyclic β-(1 → 2)-linked glucans based on NMR analysis of the β-glucans produced by *Xanthomonas campestris*. Carbohydr Res 278:205–225

Zhang L, Zhou J, Zhang L (2013) Structure and properties of β-cyclodextrin/cellulose hydrogels prepared in NaOH/urea aqueous solution. Carbohydr Polym 94:386–393. doi:10.1016/j.carbpol.2012.12.077